

tionen 17 und 18 im Heptan deutlich außerhalb der Fehlergrenzen verschieden. KLOTS zeigte, daß ein „loser“ aktivierter Komplex größere kinetische Energie ergibt. Dies, bei der sonstigen Ähnlichkeit der beiden Zerfälle, würde aber ein größeres E_z für Masse 71 erwarten lassen. Daß es in Wirklichkeit umgekehrt ist, wird auf die bei der Bildung von C_2H_6 freigesetzte Energie zurückgeführt. Sie sollte zwar vorwiegend als Schwingungsenergie erscheinen, ein Teil kann aber auch in Translationsenergie umgesetzt werden. Eine Abschätzung ergibt, daß bei der Reaktion 18 (Tab. 4) im Vergleich zu 17 ein Ener-

gieüberschuß von ca. 0,5–1,5 eV freigesetzt wird. Tab. 4 zeigt, daß davon nur 0,02 eV als kinetische Energie erscheinen.

Herrn Prof. Dr. O. OSBERGHAUS danke ich herzlich für die Anregung zu dieser Arbeit und für viele wichtige Diskussionen. Zu Dank verpflichtet bin ich auch den Herren Dr. F. DORER und Dr. J. BERKOWITZ für fruchtbare Diskussionen, sowie den Herren I. HERTEL und C. MARTIN für ihre Hilfe bei den Messungen und der Auswertung. Der Deutschen Forschungsgemeinschaft danke ich für die Bereitstellung der Mittel, die diese Arbeit ermöglichten, der Fernseh GmbH, Darmstadt für die großzügige Überlassung der Netze der Ionenquelle.

Appearance Potentials of Metastable Molecular Ions

I. HERTEL and CH. OTTINGER

Physikalisches Institut der Universität Freiburg i. Br.

(Z. Naturforschg. **22 a**, 40–47 [1967] ; received 26. Oktober 1966)

Differences between the appearance potentials of fragment ions formed a few μ secs after the ionization (so-called metastables) and normal fragment ions were measured. It is shown, however, that no immediate meaning regarding the primary fragmentation mechanism can be attached to these quantities. Instead, the experimental ionization curves of metastable and normal fragments were explained by a theoretical model which assumes 1) a linear threshold law, 2) a linear relation between the logarithm of the rate constant and the internal energy in the molecular ion, and 3) a constant density of populated states on the energy scale. In the case of HCN loss from benzonitrile ions, an excellent fit between the experimental and theoretical curves can then be achieved if it is assumed that an increase of 0.65 eV internal energy increases the rate constant by one order of magnitude. This is a surprisingly slow rise of $k(E)$, compared with the few existing calculations in other cases.

The description of the decomposition of an excited polyatomic molecular ion in terms of the quasi-equilibrium theory predicts a rapid variation of the rate constant k with the internal energy E in the ion (see for example ¹). The so-called “metastable” ions (this term is here used for fragments formed a few μ secs after the initial ionization) differ from the “normal” fragment ions (which are formed in a very short time after the ionization and constitute the ordinary mass spectrum) in that the rate constant for formation of the former is several orders of magnitude smaller than for the latter. A measurement of the relative intensities of metastable and normal fragment ions as a function of the ionizing electron energy, especially near threshold, should therefore give some indication of the variation of k with E .

¹ M. L. VESTAL, J. Chem. Phys. **43**, 1356 [1965].

² O. OSBERGHAUS and CH. OTTINGER, Phys. Lett. **16**, 121 [1965].
— CH. OTTINGER, Z. Naturforschg. **22 a**, 20 [1967].

Experimental

Our apparatus has been briefly described previously ². The ions are formed in a molecular beam of 50 μ half-width which is crossed by an electron beam from an oxide coated cathode in order to reduce the thermal electron energy spread to about 0.3 eV. The ion draw-out field of 100 V/cm produces a voltage drop of 0.5 eV across the molecular beam, so that the effective energy spread can be approximated by $\sqrt{0.3^2 + 0.5^2} = 0.6$ eV. The electron energy was increased linearly with time by means of a motor driven potentiometer at a rate of about 0.25 V/min. The “normal” fragment ions were singled out by passing the ion beam through an energy selector with 2.4 eV resolution (half-width). Fragment ions formed a certain time after ionization give up part of their kinetic energy to the neutral fragment and have therefore insufficient energy to pass the selector. The “metastable” fragment ions were measured by setting the molecular beam potential to a value m_0/m times the energy required by ions to pass the selector (m_0 = mass of reactant ion, m = fragment ion mass). At this setting, only ions formed in a 15 cm long field-



free drift space in front of the energy selector could pass the selector. These are ions formed between 2 and 6 μ secs after the ionization. A magnetic mass spectrometer placed behind the energy selector then detected both normal and metastable ions at their proper mass m .

The pressure in the drift space was 10^{-7} torr and was ascertained to be low enough for collision-induced dissociations to be negligible. This check is particularly important for fragmentations with large activation energies such as in benzonitrile. Here, near the appearance potential of the fragments, the parent ion intensity is already near its maximum, so that collision-induced dissociation even of a very small fraction of parent ions would influence the apparent metastable intensity greatly. However, admitting 10^{-5} torr of krypton did not change the relative abundances of metastables from benzonitrile, as measured near the appearance potential.

Appearance potentials were determined as follows: the logarithm of the ion current was plotted versus the uncorrected electron energy, each curve being the average of at least two runs. In order to compare two such plots, their relative scales must be adjusted in some way. Two slightly different procedures were adopted: a) In the case of similar ions with widely different appearance potentials such as rare gases or parent and normal fragment ions, the intensities were matched 5 volts above the ends of the respective approximately exponential portions of the plots. b) In the case of ions with very different intensities but similar appearance potentials (typically with normal and metastable ions) the upper portions of the plots were made to coincide. Method a) was here often not applicable, as the metastable curves did not always show the exponential part due to too low intensity. Both methods are arbitrary and not based on physical grounds; they yield, however, reproducible results and are in accordance with the conventional techniques. Moreover, the results do not depend very critically on the exact point where the curves are matched, due to the steepness of the exponential part.

Not too much confidence can be attached to the detailed curve shapes of this work. As the emission current varied by a factor of two over the used voltage range, a correction had to be applied. This correction assumes that the actually ionizing fraction of the total emission current is independent of U_{el} , which need not be true. The appearance potential differences as determined by the above methods is, however, very insensitive to small changes in the curve shape.

Results

As a general test, the difference of the ionization potentials of krypton and argon was determined first (Fig. 1); on the right, the application of the "extrapolated difference method" is demonstrated,

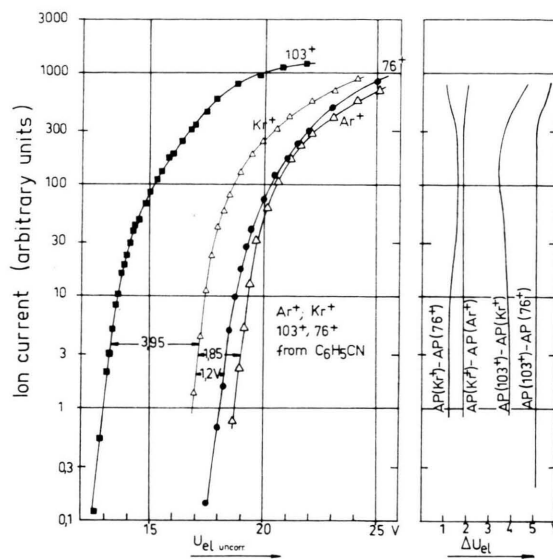


Fig. 1. Semilogarithmic plot of ion current for Kr^+ , Ar^+ , $C_6H_5CN^+$ and $C_6H_4^+$. a) vs uncorrected electron energy, b) vs electron energy difference between two ions (method of extrapolated difference).

which yields a value of $I.P.(Ar) - I.P.(Kr) = 1.85$ eV (spectroscopic value 1.76 eV³). Fig. 1 also shows curves for the parent ions of benzonitrile $C_6H_5CN^+$, mass 103, and its main fragment ion $C_6H_4^+$, mass 76. An ionization potential of benzonitrile of 8.3 eV has been determined by WALSH⁴ using a rather indirect spectroscopic argument, while MORRISON et al.⁵ found 9.95 eV using electron impact. Our value is 10.05 ± 0.2 eV. The appearance potential for $C_6H_4^+$ (normal fragment) from benzonitrile was determined from Fig. 1 as 15.2 ± 0.2 eV.

It is interesting to note that the 103^+ and 76^+ curves have a shallower rise (in the logarithmic plot) than the rare gas curves. This indicates contributions from excited ion states that become successively accessible.

Fig. 2 shows the ionization curves of two important normal fragment ions of benzonitrile along with their respective metastable curves. These were actually lower in intensity by about one to two orders of magnitude but are normalized in Fig. 2 to the normal fragment curves. It is seen that the metastables have appearance potentials 1.3 and 0.9 eV respectively below the normal fragments. These fig-

³ F. H. FIELD and J. L. FRANKLIN, *Electron Impact Phenomena*, Academic Press, New York 1957.

⁴ A. D. WALSH, *Proc. Roy. Soc. London A* **191**, 32 [1947].

⁵ J. D. MORRISON and A. J. C. NICHOLSON, *J. Chem. Phys.* **20**, 1021 [1952].

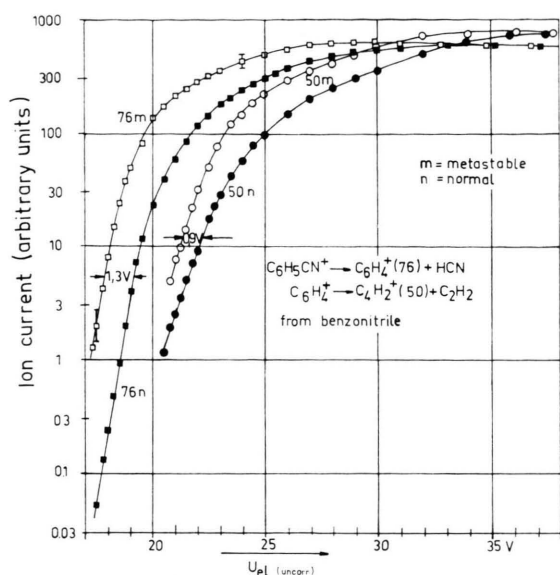


Fig. 2. Semilogarithmic plot of ion current vs uncorrected electron energy for two normal and metastable fragments from benzonitrile showing that the metastables have AP 1.3 and 0.9 eV below the normal fragments.

ures are considered accurate to within ± 0.3 eV, the main error resulting from the uncertainties of the curve shape and the normalization procedure.

A third decomposition in benzonitrile, $104^+ \rightarrow 77^+ + 27$, was also measured and gave the same curves as 76_m and 76_n , within its larger limits of error. This is as expected, since this process must also be $C_6H_5CN^+ \rightarrow C_6H_4^+ + HCN$, but with one C^{13} atom in the ions. The intensity ratio of the 76^+ and 77^+

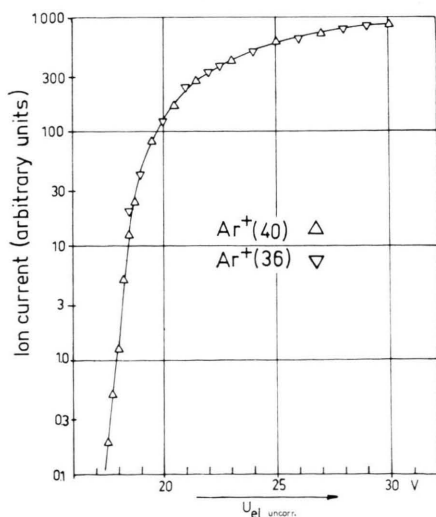


Fig. 3. Semilogarithmic plot of ion current vs uncorrected electron energy for Ar^{36} and Ar^{40} demonstrating the reliability of the method of normalization for an intensity ratio of 1:300.

metastable peaks also agreed with that calculated from the $C^{12} : C^{13}$ ratio within 20%.

In order to confirm that such surprisingly large differences of appearance potentials of metastable and normal ions are not a spurious effect caused by the normalization of so widely different intensities, a check run was carried out comparing the appearance potentials of Ar^{40} and Ar^{36} (intensity ratio 300 : 1). Fig. 3 shows the result after normalization to equal intensity in the upper range. It is seen that the curves coincide, the less abundant isotope simply not extending as far down as Ar^{40} . This gives us confidence to consider as real also other differences in appearance potentials between metastable and normal ions which were detected with butane and heptane and are shown in Figs. 4 – 6.

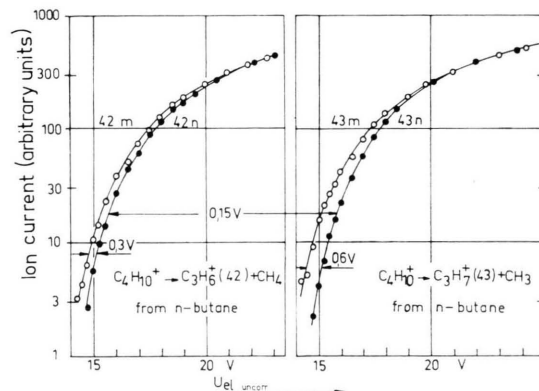


Fig. 4. Semilogarithmic plot of ion current vs uncorrected electron energy for two normal and metastable fragments from butane.

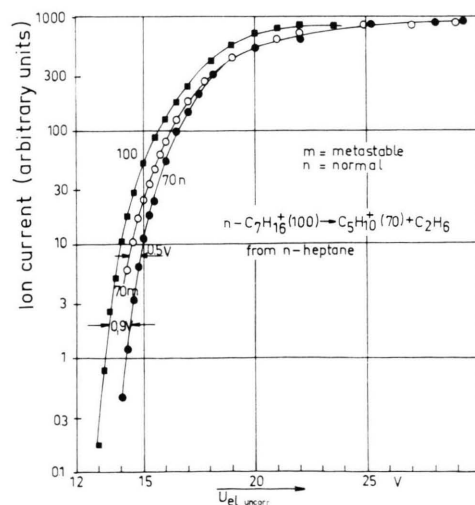


Fig. 5. Semilogarithmic plot of ion current vs uncorrected electron energy for normal and metastable mass 70 from heptane along with its parent ion.

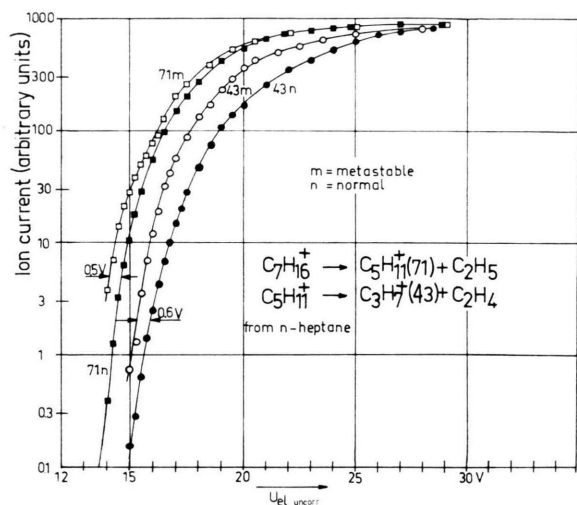


Fig. 6. Semilogarithmic plot of ion current vs uncorrected electron energy for two normal and metastable fragments from heptane.

Fig. 4 shows the curves for $C_3H_6^+$ and $C_3H_7^+$ from n-butane. Mass 42 shows a very slight difference between AP_m and AP_n , just within the limits of error, while mass 43 shows the larger difference of 0.6 eV. Mass 70 and 71 from heptane (Figs. 5 and 6) are almost identical. Fig. 5 gives again the parent ion curve which has the same shape as the parent ion curve of benzonitrile.

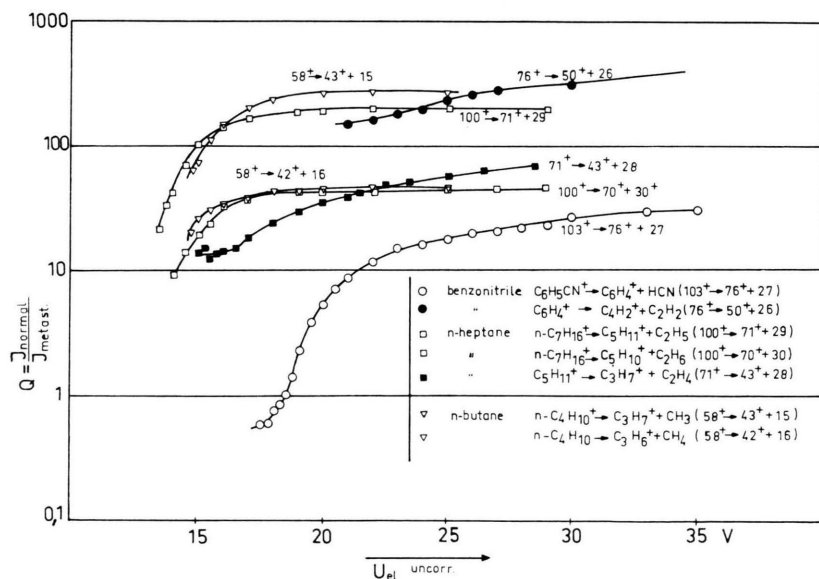


Fig. 7. Semilogarithmic plot of ratios Q_{exp} vs uncorrected electron energy for several processes in benzonitrile, butane and heptane. $Q_{exp} = (\text{True intensity of normal fragment}) : (\text{True intensity of metastable fragment})$.

Fig. 7 gives the ratios $Q_{exp} = I_n/I_m$ as a function of electron voltage in order to show the true intensities of metastables. It can be seen that $103^+ \rightarrow 76^+ + 27$ from benzonitrile gives by far the most intense metastables. Below 18 V the metastable intensity becomes even greater than the normal intensity.

Previous measurements of metastable appearance potentials have been done by FOX and LANGER⁶ with hydrocarbons and by DIBELER and ROSENSTOCK⁷ with H_2S . In⁷, metastables and normal fragments had the same appearance potential, while in⁶ small differences seemed to exist in a few cases. On the other hand, fairly large differences were found with benzene by K. R. JENNINGS and with pyridine by J. MIGNY (private communications).

Discussion

Although the comparison of ionization curves in Figs. 2, 4, 5, 6 follows a standard procedure of the literature, namely that of matching the intensities at some arbitrarily chosen voltage, this has been done merely for convenience and is not believed to form a suitable starting point for a theoretical discussion. This is because the apparent difference of the normal and metastable appearance potentials is in this representation only produced by the different

⁶ R. E. FOX and A. LANGER, J. Chem. Phys. **18**, 460 [1950].

⁷ V. H. DIBELER and H. M. ROSENSTOCK, J. Chem. Phys. **39**, 3106 [1963].

curve shapes: The metastable curves behave rather like the rare gas curves in Fig. 1, becoming linear (in a linear plot) after a fairly short curved portion, while the normal curves are made up of contributions from a wider energy range and are therefore more curved (in a linear plot; in the logarithmic plot they appear shallower). This separates them from the metastable curves, the amount of separation being determined by the voltage at which the normal curve also becomes linear. This point, however, marks the onset of secondary decompositions and therefore influences only indirectly the intensity of the fragment under study. The difference between the appearance potentials of a normal and a metastable fragment, as determined in the conventional manner, has therefore no bearing on the formation of this fragment.

For a theoretical discussion of the experimental curves one first needs to know the relative probabilities that a fragmentation with a given rate constant k will lead to the observation of the fragment as a "normal" and a "metastable" fragment, respectively. These probabilities, expressed as functions of k , clearly depend only on instrumental parameters. STEINER, GIESE and INGRAM⁸ have treated a very similar problem. The probability that a fragmentation with given k will lead to a normal fragment was calculated as the normalized overlap integral between the decay function, converted from a time

scale to a voltage scale, and the energy selector transmission curve which was centered around the voltage corresponding to $t=0$. The result is shown in Fig. 8, curve "n". It is seen that too low values of k lead to a small probability of the ion being detected as "normal" since most decompositions then occur too late for the ion energy still to be in the transmission region of the energy selector. On the other hand, $k=10^8 \text{ sec}^{-1}$ leads already to almost 100% detection efficiency, and the apparatus therefore does not distinguish between k values higher than this.

A similar curve was calculated for the metastable fragments (curve "m" in Fig. 8). The relative number of fragmentations in the field-free drift space is given simply by $e^{-kt_1} - e^{-kt_2}$, where t_1 and t_2 are the times at which the ions enter and leave the drift space. The actually measured metastable intensity is only a certain fraction of this, however, since the metastable peak on the energy scale is broadened due to excess energy set free in the decomposition⁹, so that the energy selector accepts only a "slice" out of the whole peak.

Fig. 8 was calculated for the process $103^+ \rightarrow 76^+ + 27$, but should be typical for all decompositions with not too different mass ratios.

At low k , both I_m and I_n can be shown to be proportional to k . It is interesting to note that in this region, for equal intensities I_m and I_n , k must be

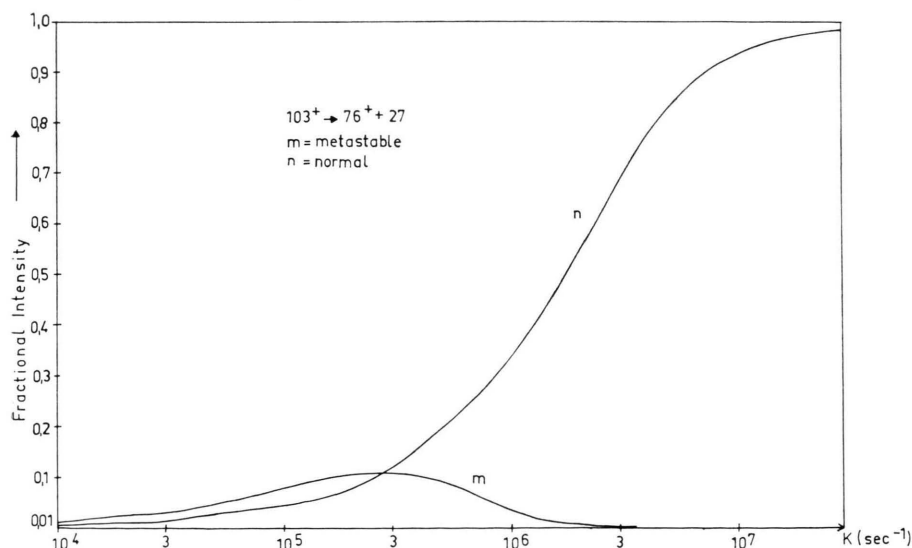


Fig. 8. Detection efficiency of the apparatus for "normal" and "metastable" ions vs rate constant k .

⁸ B. STEINER, C. GIESE, and M. INGRAM, J. Chem. Phys. **34**, 189 [1961].

⁹ CH. OTTINGER, Phys. Lett. **17**, 269 [1965].

about three times higher for the normal fragments. It is to be expected, therefore, that with increasing electron energy, the absolute metastable intensity, as measured directly with a given detection sensitivity, should rise above the noise level sooner than the normal fragment intensity, measured with the same sensitivity. A direct comparison of I_m and I_n , measured with the same sensitivity as functions of electron energy near threshold, is believed to be a less ambiguous statement than the representation in Figs. 2–6.

Since the experiment measures I_n and I_m as functions of U_{el} , Fig. 8 can only be utilized if one makes an assumption about how the excitation probability of a specific “ k -state” varies with U_{el} . The assumption made here is that this probability is proportional to the energy excess $U_{el} - E - \text{I.P.}$ over the energy E associated with the k in question (provided there exists a one-to-one relation between E and k , for example, but not necessarily, the relation predicted by the quasi-equilibrium-theory; I.P. is the ionization potential). The assumed excitation function of each k thus obeys the so-called “linear threshold law”.

The actual excitation function for a certain k_0 , $F_{k_0}(U_{el})$, deviates slightly from a straight line because of the energy spread from the thermal energy of the electrons, the molecular beam width, and the thermal energy in the molecules prior to electron impact. Taking these three factors into account, the onset of the excitation function for each k is rounded off slightly; e. g. one obtains at the threshold an ion yield that would be attained 0.15 eV above threshold if no energy spread were present. For these calculations, the thermal energy spread of the parent molecules (estimated temperature about 80 °C) was assumed to be approximately MAXWELLIAN with a mean energy near 0.2 eV⁸.

As U_{el} is increased, the increasing excitation of each specific k_0 state is described by $F_{k_0}(U_{el})$. At the same time, however, with increasing U_{el} , more and more such states become accessible. In order to calculate the total excitation, it is therefore necessary to have some knowledge of the correlation between the U_{el} -scale and the k -scale, in other words of the function $k(E)$, which is a molecular property. It is here assumed that in the vicinity of threshold $\ln k$ is proportional to E : $\ln k = \alpha \cdot E$; in the few cases in which $k(E)$ has been calculated this is a reasonable approximation over a more or less limit-

ed voltage range (see, e. g.¹). The main object of the following discussion is the determination of α . Once the assumption $\ln k = \alpha E$ has been made, $F_{k_0}(U_{el})$ is thereby converted into another function $f_{k_0}(\ln k)$, which is, like $F_{k_0}(U_{el})$, a linear function, neglecting the short exponential tail. It is to be noted here that the absolute amount in terms of eV of this tailing is fixed, so that strictly α cannot be treated as a free parameter. Since the tailing is small, and since the necessary variation of α from the first guess to the final value was found to be only about 20%, this effect was neglected.

The third important assumption that has to be made concerns the distribution of k -states. Here it is assumed that for each U_{el} the density of populated states is constant over the $\ln k$ -axis (corresponding to a density $\sim 1/k$ over the k -axis) up to k_{el} , the maximum k accessible with the given U_{el} . An experimental justification of this will be given below.

With these assumptions it is now possible to construct theoretical curves $I_{m,n}(k_{el})$ which then can be converted into curves $I_{m,n}(U_{el})$ and compared with the experimental curves. $I_{m,n}(k_{el})$ was calculated in the following way. For equidistant values of $\ln k_0$ (one half order of magnitude apart) the corresponding functions $f_{k_0}(\ln k)$ were multiplied with weighting factors given by the curves in Fig. 8 and then superimposed. The resulting sums are then the desired functions $I_{m,n}(k_{el})$.

Fig. 9 shows I_m and I_n calculated in this manner as functions of k_{el} . The abscissa extends to quite unreasonably high values of k . These arise from the extension of the linear relation $\ln k = \alpha E$ to high E and are only meant as a convenient means of numbering the highly excited states. In any case, the apparatus does not distinguish between states with k as high as this, it only records the total number of such states excited.

At the bottom of Fig. 9, the ratio $I_n/I_m = Q_{calc}$ has been plotted. This ratio can now be compared with the experimentally determined ratio Q_{exp} in Fig. 7. If the assumption $\ln k = \alpha E$ is a reasonable approximation, these two curves should be related to each other by a simple linear transformation of the abscissa. Trying this out for benzonitrile $C_6H_5CN^+ \rightarrow C_6H_4^+ + HCN$, it was found that a relation

$$\log_{10}(k) = 1.54 U_{el} - 21.7 \quad (1)$$

gave an optimal fit of Q_{calc} to Q_{exp} . The crucial test is now how well this empirical relation also fits the

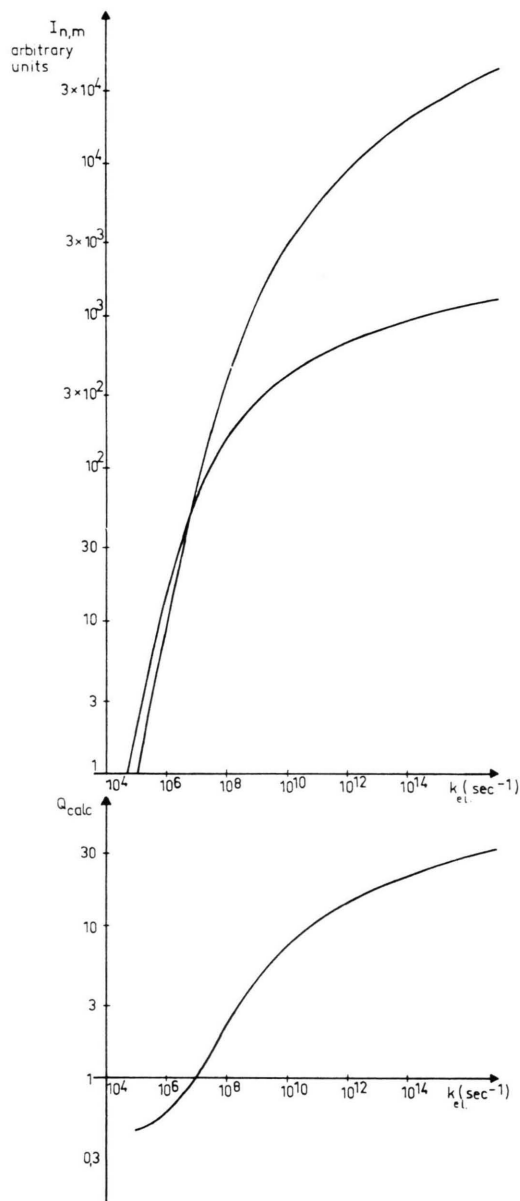


Fig. 9. Calculated ion intensities of metastables and normal fragments vs $\ln k$.

curves $I_{n, \text{calc}}$ and $I_{m, \text{calc}}$ individually to $I_{n, \text{exp}}$ and $I_{m, \text{exp}}$. In Fig. 10, the experimental points are the same as in Fig. 2, but in their correct intensity relation. The curves are derived from Fig. 9 via the transformation (1). No further fit of the calculated to the experimental curves was applied in Fig. 10 except for a simultaneous shift of both calculated curves parallel to the intensity axis, which merely relates the experimental scale divisions to the calculated intensities.

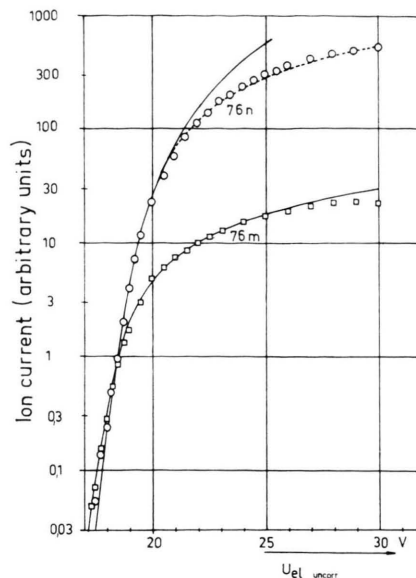


Fig. 10. Comparison of calculated and experimental intensities of metastable and normal fragment C_6H_4^+ from benzonitrile; full curve: Without secondary decompositions, broken curve: Assuming the onset of a secondary decomposition at $k = 5 \cdot 10^8 \text{ sec}^{-1}$, points: Experimental.

It is seen that near threshold an excellent fit can be obtained. Especially for I_m a discrepancy does not occur until several volts above threshold. Now, in this upper region, $I_{m, \text{calc}}$ is a linear function of U_{el} . This is because the contribution from each k is almost linear according to the first assumption made above; and from Fig. 8 it is seen that only k -states from an interval covering about two orders of magnitude, corresponding to about $2/1.54 = 1.3 \text{ eV}$, can contribute to I_m . Therefore, from 1.3 eV above threshold, I_m should depend linearly on U_{el} . Fig. 10 thus gives a justification of the assumption of a linear threshold law. Possibly the deviation starting at about 8 V above threshold indicates the breakdown of this law. Direct observations on the validity of a threshold law for metastables were made by BREHM¹⁰ using photoionization; here the threshold law should be a step function, and indeed BREHM observed that the ion yield of certain metastables in heptane increased with photon energy only for about 0.5 eV above threshold, but then became constant to within 30% for another 1.2 eV.

In contrast, $I_{n, \text{calc}}$ does not become linear, but exhibits a continually increasing slope because of more and more k -states contributing. The experimental points in Fig. 10 do not show this behavior.

¹⁰ B. BREHM, Z. Naturforschg. **21 a**, 196 [1966].

ious; from about 2–3 eV above threshold $I_{n, \text{exp}}$ follows more closely a linear function (or, in Fig. 10, a logarithmic curve). This is ascribed to the onset of secondary decompositions of C_6H_4^+ , presumably to $\text{C}_4\text{H}_2^+ + \text{C}_2\text{H}_2$. Fig. 2 shows that $\text{AP}_{76} - \text{AP}_{50} \approx 2 - 3$ eV (this difference is not very well defined, since apparently mass 50 contains two contributions from processes with different activation energies). The presence of secondary decompositions would mean that only up to a certain energy E_{max} , corresponding to a certain maximum k_{max} , new k -states leading to mass 76 would be excited. At higher energies, as far as mass 76 is concerned, only the states with $k < k_{\text{max}}$ would be excited with linearly increasing probability, in agreement with the observation.

In order to allow for these secondary decompositions in the theory, an additional calculation was carried out in which the superposition of k -states only included states up to $k = 5 \cdot 10^8 \text{ sec}^{-1}$. The result is shown by the broken line in Fig. 10 which approximates the experimental points far better. The upper region of this theoretical curve is now also a linear function (logarithmic in Fig. 10). If the maximum k at which the summation is stopped is increased by about half an order of magnitude, the upper portion of the calculated curve comes out higher by about 16%.

There is some independent experimental evidence for the existence of k_{max} . The decomposition rate of $\text{C}_6\text{H}_5\text{CN}^+ \rightarrow \text{C}_6\text{H}_4^+ + \text{HCN}$ was directly measured as a function of time down to 10^{-8} secs. The method has been described elsewhere². The result was that the decay function at high electron energy can be rather well (within $\pm 10\%$) approximated by

$$\int_0^{k_{\text{max}}} e^{-kt} dk$$

with a k_{max} of $(6 \pm 4) \cdot 10^8 \text{ sec}^{-1}$. This is in agreement with the value $5 \cdot 10^8$, determined in a completely different way as described above. It follows from the principle of these direct decomposition rate measurements² that the total decay function is a sum of contributions $k \cdot e^{-kt}$ from the individual k -states. These states must therefore in the case of benzonitrile be populated with statistical weights

proportional to $1/k$ in order to give the observed function $\int e^{-kt} dk$. This population is just the one postulated above (see assumption three).

It should be emphasized that the empirical relation (1) indicates a *surprisingly slow rise of k with E , about one order of magnitude per 0.65 eV*. This slow rise explains the high intensity of the metastables, since, as derived above from Fig. 8, an energy interval as large as 1.3 eV generates them. Intense metastables also occur in benzene¹¹, where the rise of $k(E)$ should therefore be similarly shallow. On the other hand, the large difference of appearance potentials, as demonstrated by Fig. 2, does not give evidence on $k(E)$, but only on the particularly late onset of secondary reactions, as was explained above. Benzene also has large activation energies for secondary reactions³. One might speculate that large metastable intensity [i. e. shallow $k(E)$] and large activation energies for secondary reactions are connected in some way.

All the other processes studied in this work do not allow conclusions to be drawn about $k(E)$. Here, Q_{exp} (Fig. 7) and Q_{calc} (Fig. 9) cannot be correlated by a linear transformation of the voltage scale, mainly because of the long horizontal portion which is only present in Q_{exp} . This portion means that not only I_m but also I_n depends linearly on U_{el} , the threshold for secondary processes being very low in these cases. A comparison between Q_{exp} and Q_{calc} would therefore only be possible in the region where Q_{exp} is still rising. Here, however, even the lowest values of Q_{exp} , measured at the minimum detectable I_m , are still far greater than unity. The "cross-over", where I_n becomes equal to I_m ($Q=1$), occurs at much lower I_m and is unobservable. According to Fig. 9, the smallest Q_{exp} values all correspond to $k > 10^8$, while the measurement only distinguishes between k values smaller than about 10^7 sec^{-1} . The Q_{exp} in all cases other than benzonitrile will therefore not give information about $k(E)$. The only qualitative conclusion that can be drawn from the small metastable intensity is that $k(E)$ must be very much steeper than in the case of benzonitrile.

Acknowledgment

We thank Prof. Dr. O. OSBERGHAUS for his stimulating interest in this work, as well as the Deutsche Forschungsgemeinschaft for financial support.

¹¹ CH. OTTINGER, Z. Naturforschg. **20 a**, 1229 [1965].